Eur. Phys. J. Spec. Top. (2024) 233:2075–2086
https://doi.org/10.1140/epjs/s11734-023-01006-0

THE EUROPEAN PHYSICAL JOURNAL SPECIAL TOPICS

Regular Article

Prediction of various observables for $B_s^0 \to D_s^{(*)-}\ell^+\nu_\ell$ within covariant confined quark model

J. N. Pandya[1,a], P. Santorelli[2,3,b], and N. R. Soni[3,4,c]

[1] Department of Physics, Sardar Patel University, Vallabh Vidyanagar 388120, India
[2] Dipartimento di Fisica "E. Pancini", Università di Napoli Federico II, Complesso Universitario di Monte S. Angelo Edificio 6, via Cintia, 80126 Napoli, Italy
[3] INFN sezione di Napoli, Complesso Universitario di Monte S. Angelo Edificio 6, via Cintia, 80126 Napoli, Italy
[4] Department of Physics, Faculty of Science, The Maharaja Sayajirao University of Baroda, Vadodara, Gujarat 390002, India

Received 18 July 2023 / Accepted 20 October 2023 / Published online 2 November 2023

Abstract In 2020, the LHCb collaboration reported the exclusive branching fractions for the channels $B_s^0 \to D_s^{(*)-}\mu^+\nu_\mu$ for the very first time. In view of these observations, we have recently reported the form factors and branching fraction computations for these channels employing the covariant confined quark model. As different other channels corresponding to $b \to c\ell\nu_\ell$ have provided the hint for new physics, the analysis of observables, such as forward–backward asymmetry, and longitudinal and transverse polarizations across the lepton flavours can serve as one of the important probes for the search for possible new physics. In the present work, we compute these observables for all the lepton flavors and compare our predictions with the other theoretical approaches.

1 Introduction

For the last many years, $b \to c\ell\nu_\ell$ has served as a very precise probe for the search of new physics. As both the quarks involved in this transition are heavy, it has great phenomenological implications within and beyond the standard model. Experimentally, precise results are available for the channels $B \to D^{(*)}\ell\nu_\ell$ through different facilities such as BABAR, BELLE and LHCb collaborations. Precise lattice results are also available corresponding to these transitions [1, 2]. Different heavy flavor anomalies corresponding to these transitions are reported in Ref. [3–5] and references therein. Similarly, $B_s \to D_s^{(*)}\ell\nu_\ell$ can also serve as a prominent channel for understanding the heavy flavor dynamics and possibly the anomalies. On the experimental side, LHCb have reported the branching fractions for the channels $B_s^0 \to D_s^{(*)-}\mu\nu_\mu$ for the very first time [6] and determined the ratio of the branching fractions $B_s^0 \to D_s^-\mu^+\nu_\mu$ to $B_s^0 \to D_s^{*-}\mu^+\nu_\mu$. Additionally, they also determined the ratios of these branching fractions relative to $B \to D$, namely,

$$\frac{\mathcal{B}(B_s^0 \to D_s^-\mu^+\nu_\mu)}{\mathcal{B}(B^0 \to D^-\mu^+\nu_\mu)} = 1.09 \pm 0.05_{\rm stat} \pm 0.06_{\rm syst} \pm 0.05_{\rm ext}$$
$$\frac{\mathcal{B}(B_s^0 \to D_s^{*-}\mu^+\nu_\mu)}{\mathcal{B}(B^0 \to D^{*-}\mu^+\nu_\mu)} = 1.06 \pm 0.05_{\rm stat} \pm 0.07_{\rm syst} \pm 0.05_{\rm ext}.$$

The ratios of the decay widths from tau mode to electron mode for $D_s^{(*)}$ ($R(D_s)$ and $R(D_s^*)$) are yet to be measured experimentally so far. However, lattice results are available for these ratio in the Refs. [7, 8]. New physics studies have also been reported using these lattice form factors in Ref. [9]. Recently, the ratios $R(D_s^{(*)})$ have been computed using unitarity and lattice QCD approach [10], where the transition form factors are computed in the entire momentum transfer range using the dispersive matrix approach. The transition form factors, branching fractions and ratios $R(D_s^{(*)})$ are also computed using three point QCD sum rules [11, 12]

[a] e-mail: jnpandya-phy@spuvvn.edu
[b] e-mail: pietro.santorelli@na.infn.it
[c] e-mails: nakulphy@gmail.com; nakul.soni@na.infn.it (corresponding author)

and also using light cone QCD sum rules in the framework of heavy quark effective theory [13, 14]. Transition form factors, branching fractions and other observables have also been computed recently within the framework of relativistic quark model (RQM) based on the quasipotential approach in QCD [15, 16]. The transition form factors are also computed in both space- and time-like momentum transfer range within the constituent quark model framework [17], employing the next-to-leading-order QCD corrections [18] and also employing light front quark model (LFQM) [19]. Heavy to heavy and heavy to light semileptonic transitions form factors are also computed employing the symmetry preserving vector–vector contact interactions (SCI) [20]. The detailed descriptions of transition form factors and branching fractions are available in literature; however, the detailed analysis of other physical observables such as forward–backward asymmetry and different polarizations observables are yet to be explored. As there is no indication of these observables from the experimental side, they may also serve as crucial probes for search for the physics beyond the standard model. In the theoretical side, there are very few references in which these observables are studied, with few of them being lattice results [8], RQM [15] and light cone QCD sum rules [13]. These observables are also studied considering the new physics scenario [21–23].

Very recently, we have studied the transition form factors, branching fractions of these channels, namely, $B_s \to D_s^{(*)}\ell\nu_\ell$ with $\ell = e,\ \mu$ and τ within the quark model framework [24]. In this work, we have reported detailed analysis of the branching fractions with the recent LHCb data and it is observed that our results are in excellent agreement with them along with lattice and other theoretical models. In this paper, we provide a much detailed description of the form factors with comparison to the lattice and other theoretical approaches. We also provide detailed plots for the different physical observables such as forward–backward asymmetries, longitudinal and transverse polarization, lepton and hadron side convexity parameter and so on. Together with [24], this work will provide complete description of the dynamics of semileptonic $B_s \to D_s^{(*)}$ decays.

The rest of the paper is organized in the following way. After a brief introduction and some very recent literature survey, for computation of the transition form factors, we provide a very short description to our theoretical model that is covariant confined quark model in Sect. 2 and provide the form factors in the double pole approximation. We also compare our results with other theoretical approaches. Next in Sect. 3, we give the relations for the computation of the different physical observables. We also provide the plots of these observables as well as the expectation values of these observables. In Sect. 4, we discuss about all the results obtained for the semileptonic decay for the channels $B_s^0 \to D_s^{(*)-}\ell^+\nu_\ell$ for $\ell = e,\ \mu,\ \tau$. Finally, we conclude the present work in Sect. 5.

2 Form factors

Within the framework of the standard model, the matrix element for the semileptonic transition can be in the general form as

$$\begin{aligned}\mathcal{M}(M_1 \to M_2^{(*)}\ell^+\nu_\ell) \\ = \frac{G_F}{\sqrt{2}} V_{\rm CKM}\langle M_2^{(*)}|\bar{q}_2 O^\mu q_1|M_1\rangle[\ell^+ O_\mu \nu_\ell].\end{aligned} \tag{1}$$

This transition matrix element can also be parametrized in terms of form factors as

$$\begin{aligned}&\langle M_2(p_2)|\bar{q}_2 O^\mu q_1|M_1(p_1)\rangle \\ &\quad = F_+(q^2)P^\mu + F_-(q^2)q^\mu, \\ &\langle M_2^*(p_2,\,\epsilon_\nu)|\bar{q}_2 O^\mu q_1|M_1(p_1)\rangle = \frac{\epsilon_\nu^\dagger}{m_{M_1}+m_{M_2}} \\ &\quad \times \big[-g^{\mu\nu}P\cdot q A_0(q^2) + P^\mu P^\nu A_+(q^2) \\ &\quad + q^\mu P^\nu A_-(q^2) + i\varepsilon^{\mu\nu\alpha\beta}P_\alpha q_\beta V(q^2)\big].\end{aligned} \tag{2}$$

In the above equations, G_F is the Fermi coupling constant and $O^\mu = \gamma_\mu(1-\gamma_5)$ is the weak Dirac matrix. Also, $P = p_1 + p_2$, $q = p_1 - p_2$ and ϵ_ν are the polarization vector. Further, the on-shell conditions demand $p_1^2 = m_{M_1}^2$ and $p_2^2 = m_{M_2}^2$. The form factors appearing in these equations are computed employing the effective field theoretical approach of covariant confined quark model (CCQM) originally developed by M. A. Ivanov and G. V. Efimov [25–31]. The hadronic interaction Lagrangian can be written as

$$\begin{aligned}\mathcal{L}_{\rm int} =& g_M M(x)\int dx_1 \int dx_2 \\ &\times F_M(x;x_1,\,x_2)\bar{q}_2(x_2)\Gamma_M q_1(x_1) + \text{H.c.}\end{aligned} \tag{3}$$

The above Lagrangian describes the interaction of meson with the constituents. Here, the Dirac matrix Γ is the gamma matrix according the meson. $F_M(x;x_1,\,x_2)$ is the vertex function which essentially describes the distribution of quarks inside the hadron. In CCQM, for computation of different observables, we consider the Gaussian form of the vertex function. It is important to note here that there are other forms of the vertex function also, but it is observed that the physical observables are not dependent on the detailed structure of the vertex functions. Further, Gaussian form also makes the analytical work more convenient [32, 33]. In Eq. 3, g_M is the coupling constant of meson computed employing the compositeness conditions [34, 35]. The computation of g_M includes the renormalization of the self-energy diagram. This condition essentially confirms that the final mesonic state does not contain any free quark and all the quarks are confined within the hadron. Further, the matrix element of the meson mass operator and semileptonic transition form factors are described by the convolution of the Feynman propagators and Gaussian vertex functions. To have the loop integration in a

Table 1 Form factors and double pole parameters found in Eq. 2 [24]

F	$F(0)$	a	b	F	$F(0)$	a	b
$F_+^{B_s\to D_s}$	0.770 ± 0.066	0.837	0.077	$F_-^{B_s\to D_s}$	-0.355 ± 0.029	0.855	0.083
$A_+^{B_s\to D_s^*}$	0.630 ± 0.025	0.972	0.092	$A_-^{B_s\to D_s^*}$	-0.756 ± 0.031	1.001	0.116
$A_0^{B_s\to D_s^*}$	1.564 ± 0.065	0.442	-0.178	$V^{B_s\to D_s^*}$	0.743 ± 0.030	1.010	0.118

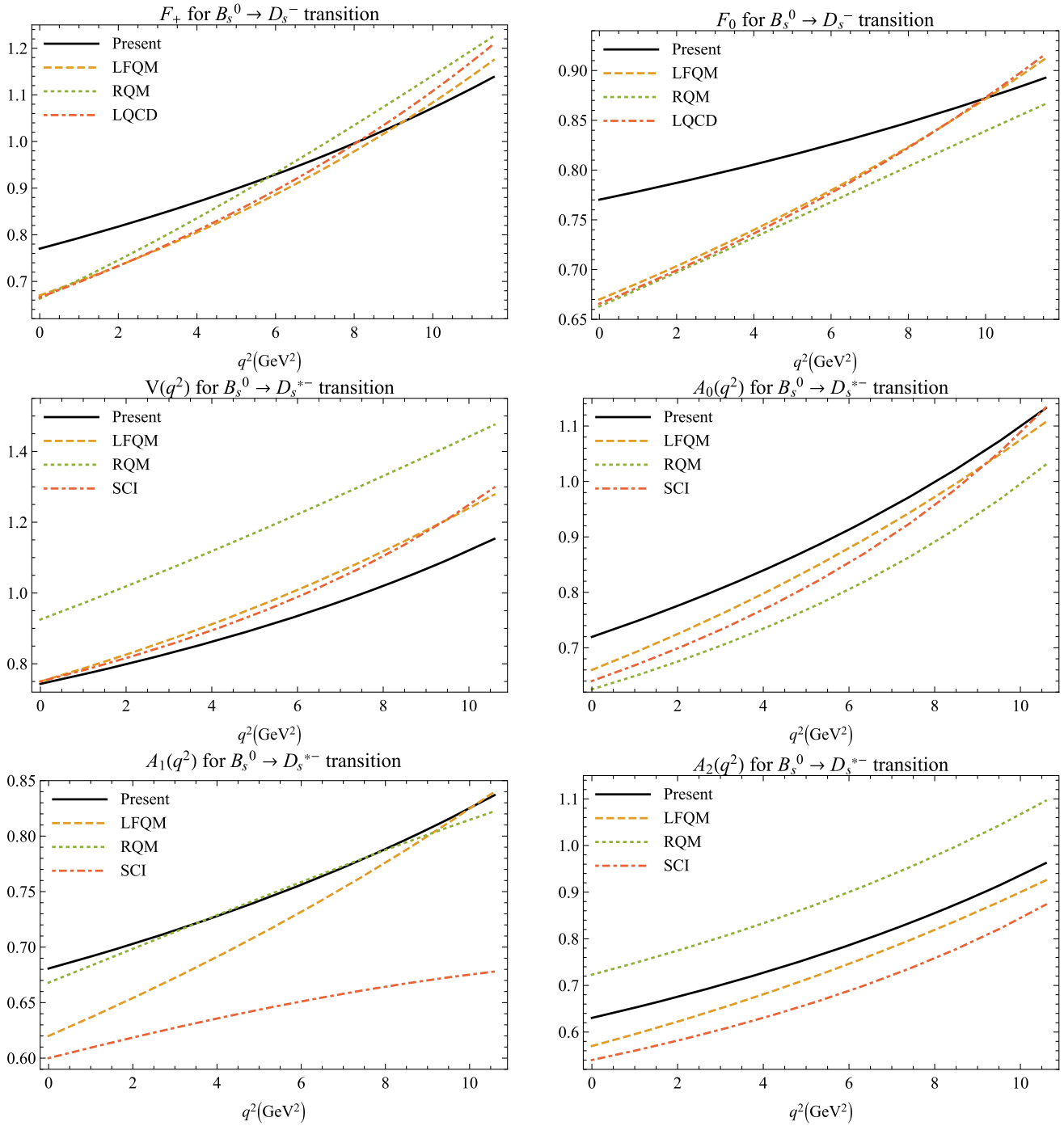

Fig. 1 Form factors in comparison with LFQM [19], RQM [15], LQCD [7] and SCI [20]

more efficient way, we use the Fock Schwinger representation of the Feynman propagator. Finally, to overcome any ultraviolet divergences appearing in the diagrams, we introduce the infrared cutoff parameter $\lambda = 0.181$ GeV. Note here that we take λ to be same for all the physical processes studied using the CCQM.

There are only two other model parameters, namely quark mass and size parameter, which are fixed by fitting with some basic properties such as leptonic decay widths with the available experimental data or lattice simulations. The parametrization is also achieved in such a way that the deviation in the decay width computation remains minimum. The uncertainties in the fitted size parameters are determined from the differences in the predicted and experimental data. It is interesting to note here that the observed uncertainness are found to be less than 5% for all the mesonic cases. These uncertainties are then transported into the computation of all the observables such as form factors and then branching fractions and other physical observables. It is observed that the uncertainties are less than 5% at the $q^2 = 0$ and less than 10% for $q^2 = q^2_{\rm max}$. The propagation of uncertainty in any observables can be computed using the most general technique. For instance, the uncertainty propagation in the forward–backward asymmetry for the transition corresponding to the channel $B_s^0 \to D_s^-$ can be written as [36]

$$\Delta(A_{\rm FB}(q^2)) = \sqrt{\sum_{i=+,-}\left(\frac{\partial(A_{\rm FB}(q^2))}{\partial F_i}\Delta F_i\right)^2}. \quad (4)$$

Here, ΔF_i is the uncertainty in the form factor. For all the finer details regarding the computational techniques, we suggest the readers to refer to [28, 37].

We also present the form factors Eq. (2) in the double pole approximation form. The relation reads

$$F(q^2) = \frac{F(0)}{1 - a\left(\frac{q^2}{m^2_{M_1}}\right) + b\left(\frac{q^2}{m^2_{M_1}}\right)^2}. \quad (5)$$

The parameters a and b and the form factor $F(0)$ are listed in Table 1. We also transform our form factors with the Bauer–Stech–Wirbel form factors [38] so that we can have a brief comparison of our form factors in the entire q^2 range with different other theoretical approaches such as light front quark model [19], relativistic quark model [16] and lattice simulations [7]. The transformed (primed) form factors read

$$\begin{aligned} F_0' &= F_+ + \frac{q^2}{m^2_{M_1} - m^2_{M_2}}F_-, \qquad F_+' = F_+ \\ A_0' &= \frac{m_{M_1} - m_{M_2}}{2m_{M_2}}\left(A_0 - A_+ - \frac{q^2}{m^2_{M_1} - m^2_{M_2}}A_-\right), \\ A_1' &= \frac{m_{M_1} - m_{M_2}}{m_{M_1} + m_{M_2}}A_0, \qquad A_2' = A_+, \qquad V' = V. \end{aligned} \quad (6)$$

Note that to avoid confusion, we will not use prime from now on. In Fig. 1, we compare transition form factors $F_+(q^2)$ and $F_0(q^2)$ with light front quark model, relativistic quark model and also the lattice simulations.

CCQM is a very versatile model and can be employed for studying not only mesons and baryons, but also mutiquark states as well. In the last few years, we have employed CCQM for studying the semileptonic decays of charmed mesons [31, 36, 39–43], bottom-strange mesons [24] and rare semileptonic decays of bottom mesons [44–46]. Ivanov et. al. have also utilized CCQM for computation of various decay properties of B, B_s and B_c mesons in Ref. [29, 47–55].

3 Different physical observables

After computation of transition form factors, we compute various other physical observables such as forward–backward asymmetry, lepton-side convexity parameter, and longitudinal and transverse polarization. In Ref. [24], we have computed the semileptonic branching fractions and made a detailed comparison with the LHCb data, and here in the present work, we compute some other physical observables that are yet to be identified by the experimental facilities worldwide. These observables are forward–backward asymmetry, convexity parameter, longitudinal and transverse polarization of charged leptons, and longitudinal polarization fractions of daughter vector meson. In semileptonic decays, these observables are dependent on the lepton masses and therefore these observables are very important probes to understand the effects of lepton masses. In the present work, we use the same notations used for studying the semileptonic D and D_s decays [31]. We compute the following physical observables in the entire q^2 range and their relations are defined as [16, 56–58]:

1. Forward–backward asymmetry:

$$A_{\rm FB}(q^2) = \frac{3}{4}\frac{\mathcal{H}_P - 2\frac{m_\ell^2}{q^2}\mathcal{H}_{SL}}{\mathcal{H}_{tot}}. \quad (7)$$

2. Lepton-side convexity parameter:

$$C_F^\ell = \frac{3}{4}\left(1 - \frac{m_\ell^2}{q^2}\right)\frac{\mathcal{H}_U - 2\mathcal{H}_L}{\mathcal{H}_{tot}}. \quad (8)$$

3. Longitudinal polarization of charged leptons:

$$P_L^\ell = \frac{(\mathcal{H}_U + \mathcal{H}_L)\left(1 - \frac{m_\ell^2}{2q^2}\right) - \frac{3m_\ell^2}{2q^2}\mathcal{H}_s}{\mathcal{H}_{tot}}. \quad (9)$$

Table 2 Averages of different physical observables for $B_s^0 \to D_s^- \ell^+ \nu_\ell$ channel

Observable	$-\langle A_{FB}^e\rangle \times 10^{-6}$	$-\langle A_{FB}^\mu\rangle$	$-\langle A_{FB}^\tau\rangle$	$-\langle C_F^e\rangle$	$-\langle C_F^\mu\rangle$	$-\langle C_F^\tau\rangle$
Present	1.156 ± 0.295	0.015 ± 0.004	0.362 ± 0.113	1.500 ± 0.395	1.455 ± 0.384	0.260 ± 0.079
RQM [16]	0.97	0.013	0.36	1.5	1.46	0.3
Observable	$\langle P_L^e\rangle$	$\langle P_L^\mu\rangle$	$-\langle P_L^\tau\rangle$	$-\langle P_T^e\rangle \times 10^{-3}$	$-\langle P_T^\mu\rangle$	$-\langle P_T^\tau\rangle$
Present	1.000 ± 0.263	0.958 ± 0.253	0.337 ± 0.119	1.115 ± 0.294	0.205 ± 0.054	0.839 ± 0.264
RQM [16]	1.000	0.960	0.27	1.02	0.19	0.85

Table 3 Averages of different physical observables for $B_s^0 \to D_s^{-*} \ell^+ \nu_\ell$ channel

Observable	$-\langle A_{FB}^e\rangle$	$-\langle A_{FB}^\mu\rangle$	$-\langle A_{FB}^\tau\rangle$	$-\langle C_F^e\rangle$	$-\langle C_F^\mu\rangle$	$-\langle C_F^\tau\rangle$
Present	0.195 ± 0.024	0.201 ± 0.025	0.284 ± 0.037	0.452 ± 0.089	0.436 ± 0.086	0.060 ± 0.012
RQM [16]	0.26	0.27	0.32	0.35	0.33	0.040
Observable	$\langle P_L^e\rangle$	$\langle P_L^\mu\rangle$	$\langle P_L^\tau\rangle$	$-\langle P_T^e\rangle \times 10^{-3}$	$-\langle P_T^\mu\rangle$	$-\langle P_T^\tau\rangle$
Present	1.000 ± 0.148	0.985 ± 0.145	0.504 ± 0.067	0.322 ± 0.063	0.058 ± 0.011	0.126 ± 0.034
RQM [16]	1.000	0.990	0.530	0.23	0.040	0.035
Observable	$\langle F_L^e\rangle$		$\langle F_L^\mu\rangle$	$\langle F_L^\tau\rangle$		
Present	0.534 ± 0.088		0.534 ± 0.088	0.458 ± 0.070		
RQM [16]	0.49		0.49	0.42		
LQCD [8]	–		–	0.440 (16)		

4. Transverse polarization of charged leptons:

$$P_T^\ell = -\frac{3\pi m_\ell}{8\sqrt{q^2}} \frac{\mathcal{H}_P + 2\mathcal{H}_{SL}}{\mathcal{H}_{tot}}. \tag{10}$$

5. Longitudinal polarization fraction for the final vector meson:

$$F_L(q^2) = \frac{\mathcal{H}_L\left(1 + \frac{m_\ell^2}{2q^2}\right) + \frac{3m_\ell^2}{2q^2}\mathcal{H}_S}{\mathcal{H}_{tot}}. \tag{11}$$

Using the above Eq. (11), one can also compute the transverse polarization vector of the final vector mesons via relation $F_T = 1 - F_L$. In these relations, $\mathcal{H}'s$ are the bilinear combinations of the helicity components of the hadronic tensors related to the helicity amplitudes (H) as [16, 56–58],

$$\begin{aligned} \mathcal{H}_U &= |H_+|^2 + |H_-|^2, \qquad \mathcal{H}_P = |H_+|^2 - |H_-|^2, \\ \mathcal{H}_L &= |H_0|^2, \qquad \mathcal{H}_S = |H_t|^2, \\ \mathcal{H}_{SL} &= Re(H_0 H_t^\dagger). \end{aligned} \tag{12}$$

Here, the helicity amplitudes are related to the transition form factors computed using CCQM. The relations read

1. For $B_s^0 \to D_s^-$ transitions

$$\begin{aligned} H_t &= \frac{1}{\sqrt{q^2}}(PqF_+ + q^2 F_-), \\ H_\pm &= 0 \quad and \quad H_0 = \frac{2m_{M_1}|\mathbf{p_2}|}{\sqrt{q^2}} F_+. \end{aligned} \tag{13}$$

2. For $B_s^0 \to D_s^{-*}$ transitions,

$$\begin{aligned} H_t &= \frac{1}{m_{M_1} + m_{M_2}} \frac{m_{M_1}|\mathbf{p_2}|}{m_{M_2}\sqrt{q^2}} \\ &\quad \times \left((m_{M_1}^2 - m_{M_2}^2)(A_+ - A_-) + q^2 A_-\right) \\ H_\pm &= \frac{1}{m_{M_1} + m_{M_2}} (-(m_{M_1}^2 - m_{M_2}^2)A_0 \\ &\quad \pm 2m_{M_1}|\mathbf{p_2}|V) \\ H_0 &= \frac{1}{m_{M_1} + m_{M_2}} \frac{1}{2m_{M_2}\sqrt{q^2}} \\ &\quad \times (-(m_{M_1}^2 - m_{M_2}^2)(m_{M_1}^2 - m_{M_2}^2 - q^2)A_0 \\ &\quad + 4m_{M_1}^2 |\mathbf{p_2}|^2 A_+). \end{aligned} \tag{14}$$

Here, the form factors are defined in Eq. (1). Also, the $|\mathbf{p_2}| = \lambda^{1/2}(m_{M_1}^2, m_{M_2}^2, q^2)/2m_{M_1}$ is the momentum of the $D_s^{(*)-}$ meson in the rest frame of B_s^0 mesons and λ is the Källen function. Further, in all these equations M_1 is the parent meson (B_s^0) and M_2 is the daughter meson ($D_s^{(*)-}$). Using these relations, we compute the

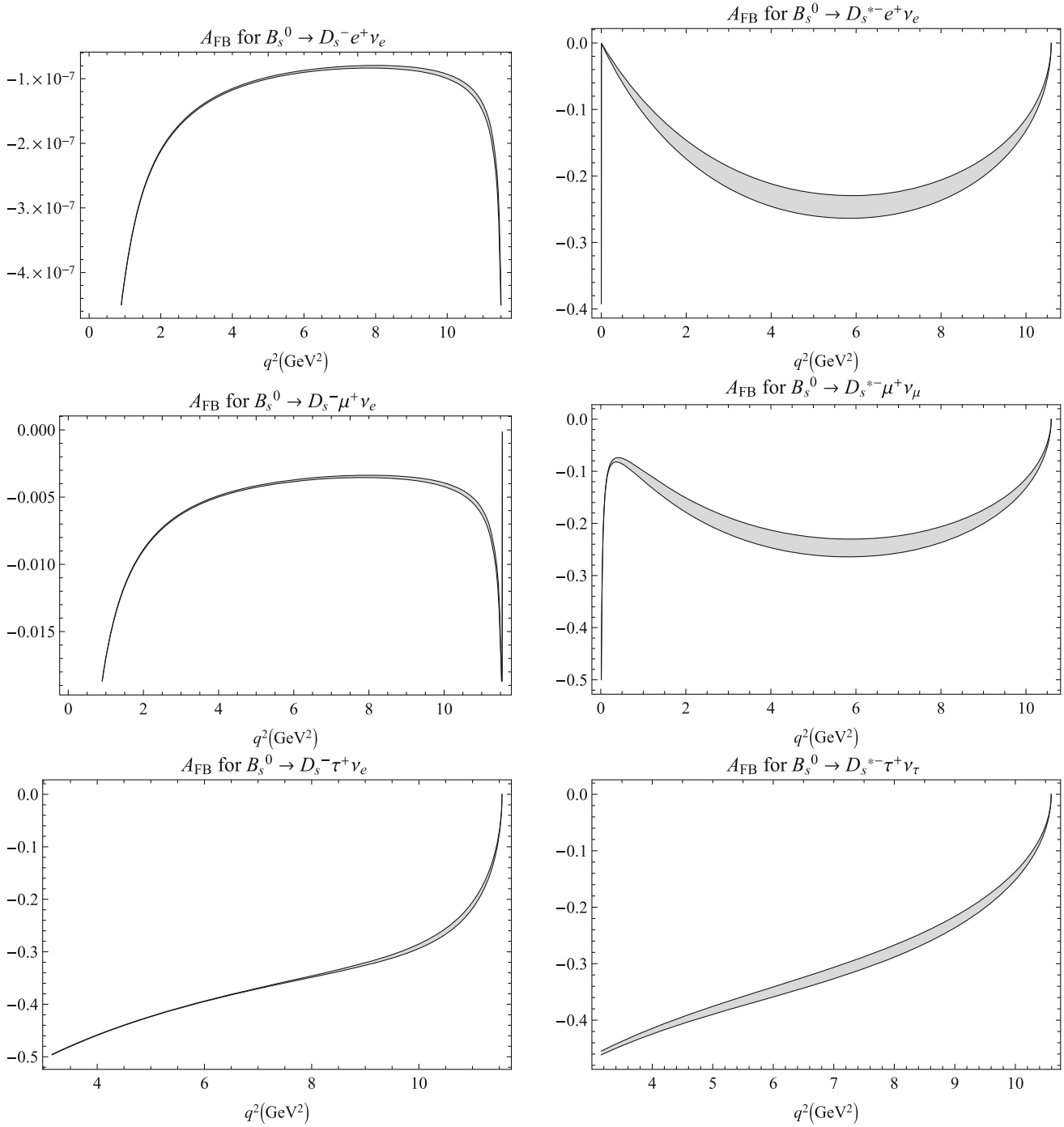

Fig. 2 Forward backward asymmetries for the decay channels $B_s^0 \to D_s^{(*)-} \ell^+ \nu_\ell$

physical observables as listed in Tables 2 and 3. We also compare our findings with the relativistic quark model predictions [16]. Note here that to compute the expectation values of these observables, one has to multiply with the phase factor $|\mathbf{p_2}|(q^2 - m_\ell^2)q^2$ to the numerator and denominator and integrate separately. The CCQM model parameters used for the present computations are quark masses $m_b = 5.05$ GeV, $m_c = 1.672$ GeV, $m_s = 0.428$ GeV and meson size parameters $\Lambda_{B_s} = 2.05 \pm 0.014$ GeV, $\Lambda_{D_s} = 1.75 \pm 0.035$ GeV and $\Lambda_{D_s^*} = 1.56 \pm 0.014$ GeV [24].

4 Results and discussion

Having determined the model parameters, namely quark masses and size parameters, we compute the transition form factors as per Eq. (2) in the entire q^2 range. In Fig. 1, we plot the form factors and also compare our form factors with light front quark model [19], relativistic quark model [16], SCI [20] as well as with the lattice simulations [7]. For $B_s^0 \to D_s^-$ form factors, our results are very near to other theoretical

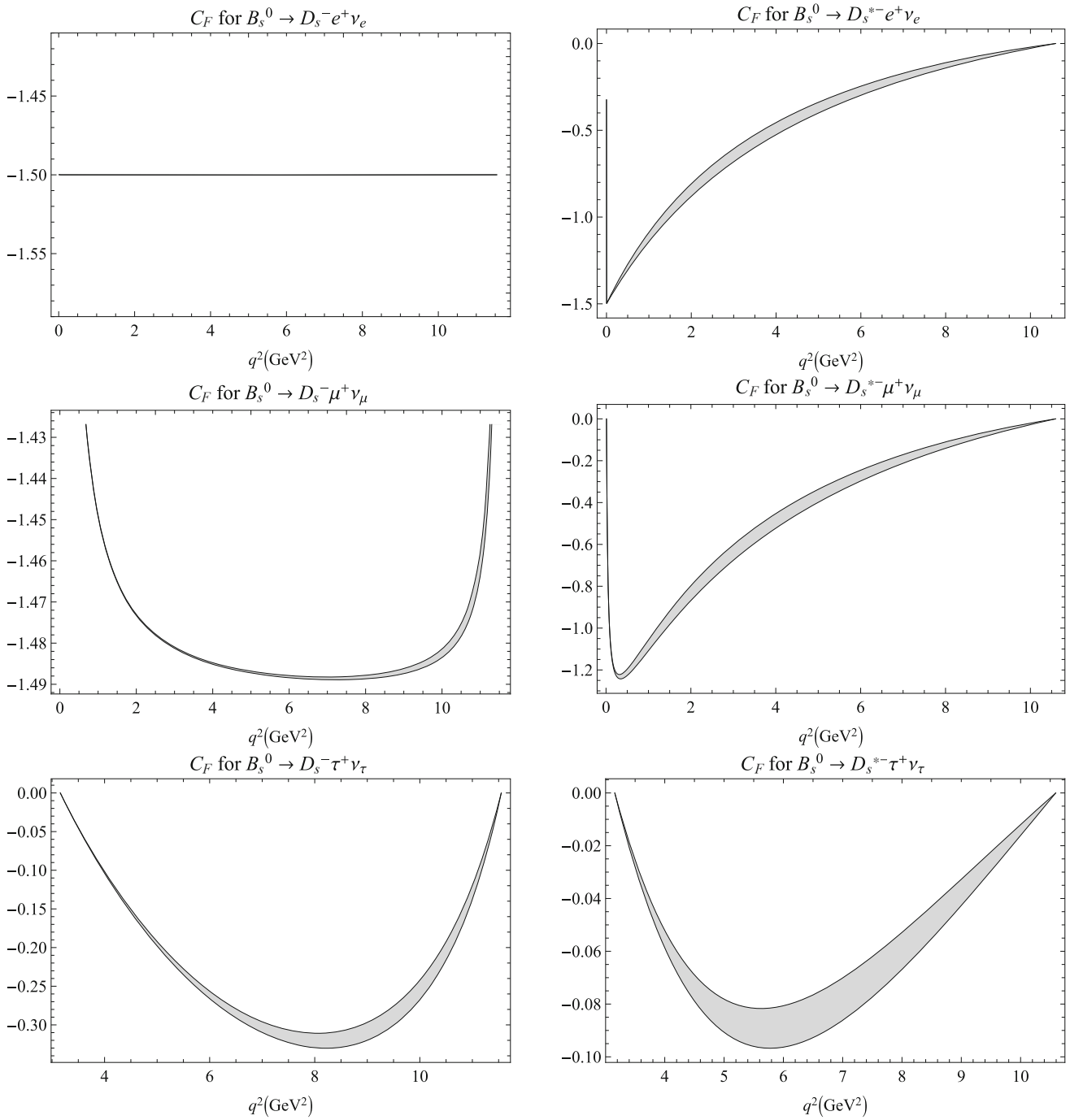

Fig. 3 Lepton-side convexity parameter for the decay channels $B_s^0 \to D_s^{(*)-} \ell^+ \nu_\ell$

approaches including lattice simulations. However, for $F_0(q^2 < 10\text{GeV}^2)$, our form factors are significantly higher than those of the other approaches. Our results for vector form factors are in very good agreement with those of other approaches.

Using the transition form factors, we compute different physical observables using the relations Eq. (7–11) and their expectation values are listed in Tables 2 and 3. These observables are yet to be identified experimentally; however, for $B \to D^{(*)}$ transitions, these observables are studied extensively by the B factories. Therefore, these observables are also expected for $B_s \to D_s^{(*)-}$ transitions from the experiments and these channels are much similar to that of $B \to D^{(*)}$ except for the spectator quark. We also compare our results with the predictions using the relativistic quark model by Faustov et al., [16] and it is observed that our results are in excellent agreement with them for all the observables. This agreement is expected, as our form factors also nearly match well. In Figs. 2, 3, 4, 5 and 6, we also

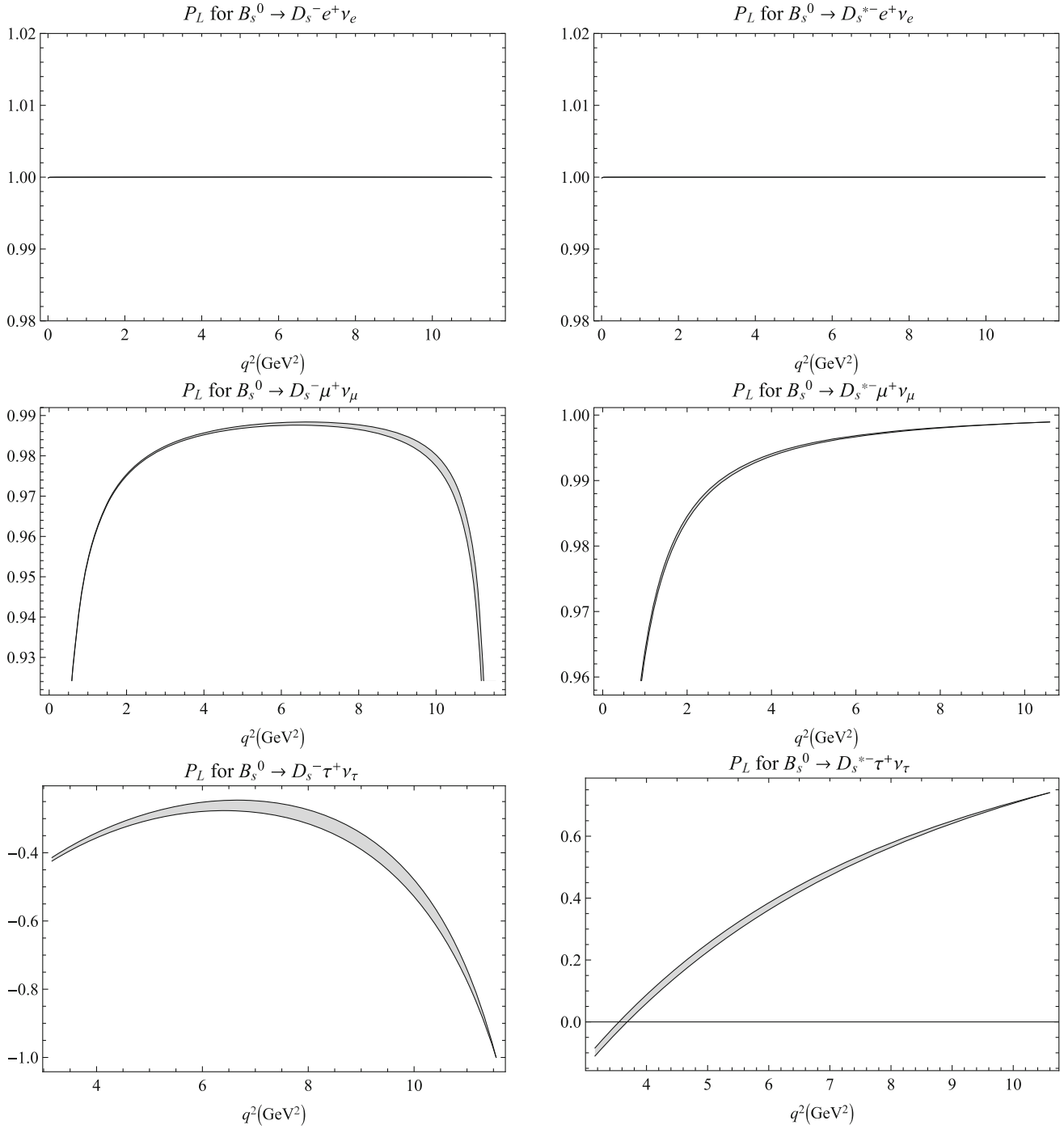

Fig. 4 Longitudinal polarization of charged leptons for the decay channels $B_s^0 \to D_s^{(*)-} \ell^+ \nu_\ell$

plot all these observables in the whole kinematical range of momentum transfer squared along with the spread of uncertainty. It is observed that the lepton-side convexity parameter for the channel $B_s^0 \to D_s^- e^+ \nu_e$ and longitudinal polarization for the channels $B_s^0 \to D_s^{(*-)} e^+ \nu_e$ are found to be constant throughout the whole q^2 range and also their spread in the uncertainty is also found to be very small and constant. Recently, HPQCD collaboration [8] have also provided the results on longitudinal polarization fraction for the $D_s^{(*)-}$ meson, and from Table 3 it is observed that our results are in excellent agreement with them. It is interesting to note here that the lepton-side convexity parameter for the channel $B_s^0 \to D_s^- e^+ \nu_e$ and longitudinal polarization of charged leptons for the channel $B_s^0 \to D_s^{(*)-} e^+ \nu_e$ are

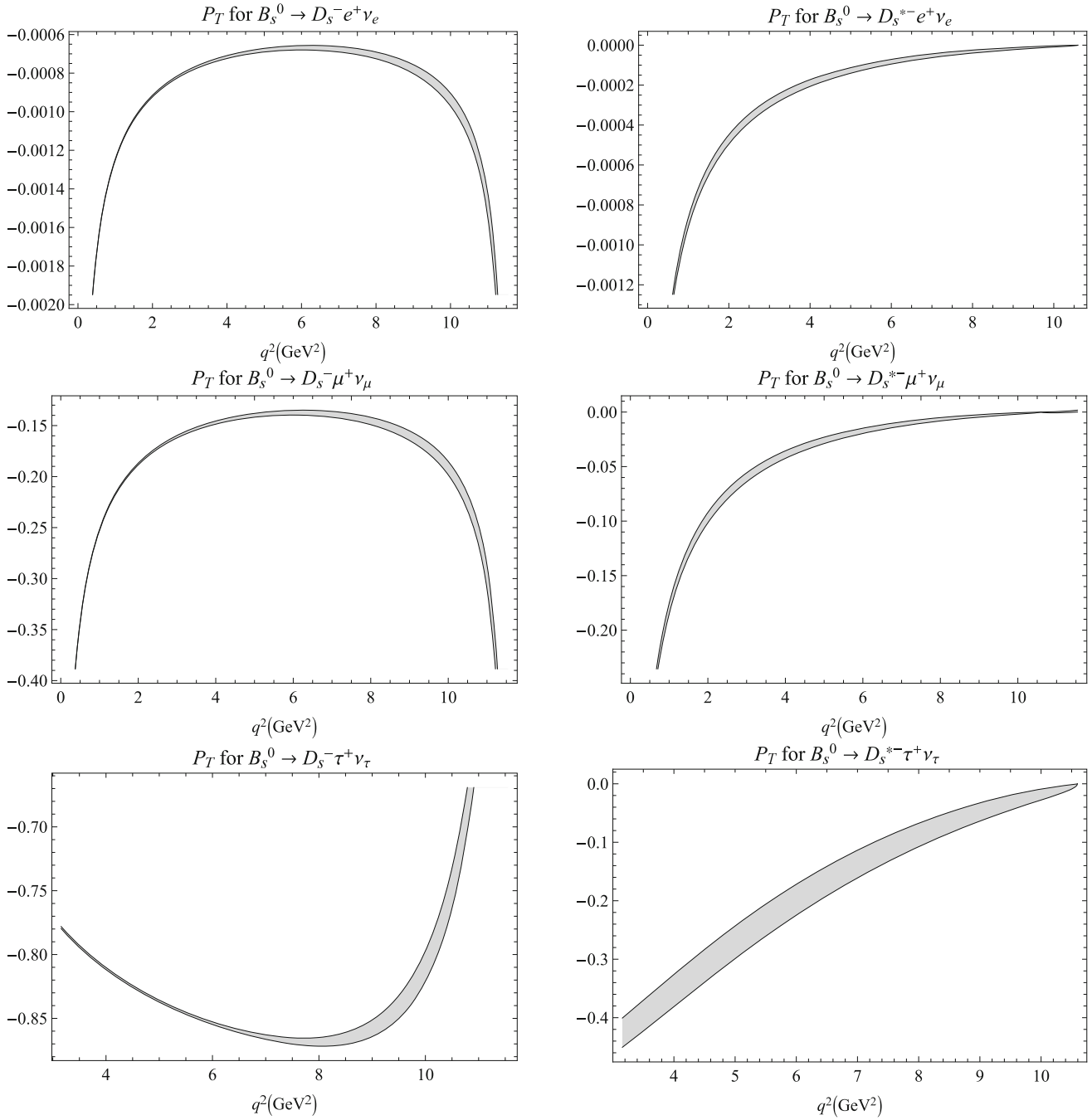

Fig. 5 Transverse polarization of charged leptons for the decay channels $B_s^0 \to D_s^{(*)-} \ell^+ \nu_\ell$

found to be constant throughout the q^2 range. This nature is also observed in the RQM predictions [16].

In our previous study [24], we have reported the semileptonic branching fractions and also provided detailed comparison with the recent LHCb measurements as well as with the lattice simulation results. We determined the normalized decay rates for the channel $B_s^0 \to D_s^{*-} \mu^+ \nu_\mu$ in the recoil parameter bins and found them to be in very good agreement with the LHCb as well as lattice results. We also determined the ratios $R(D_s) = 0.271 \pm 0.069$ and $R(D_s^{*-}) = 0.240 \pm 0.034$ and they were in very good agreement with the other theoretical approaches and lattice simulations within the uncertainties [24]. These ratios are also in agreement with the other channels concerning the transition $b \to c\tau\nu_\tau / b \to c\mu\nu_\mu$ such as $B \to D^{(*)}\ell\nu_\ell$ [59] and $B_c \to (\eta_c,\ J/\psi)\ell\nu_\ell$ [60] studied employing CCQM. Further, the ratio $\mathcal{B}(B_s^0 \to D_s^- \mu^+ \nu_\mu)/\mathcal{B}(B_s^0 \to D_s^{*-} \mu^+ \nu_\mu) = 0.451 \pm 0.096$ is also found to be in excellent agreement with the LHCb data [24]. Overall, all the results presented employing CCQM are in very good agreement

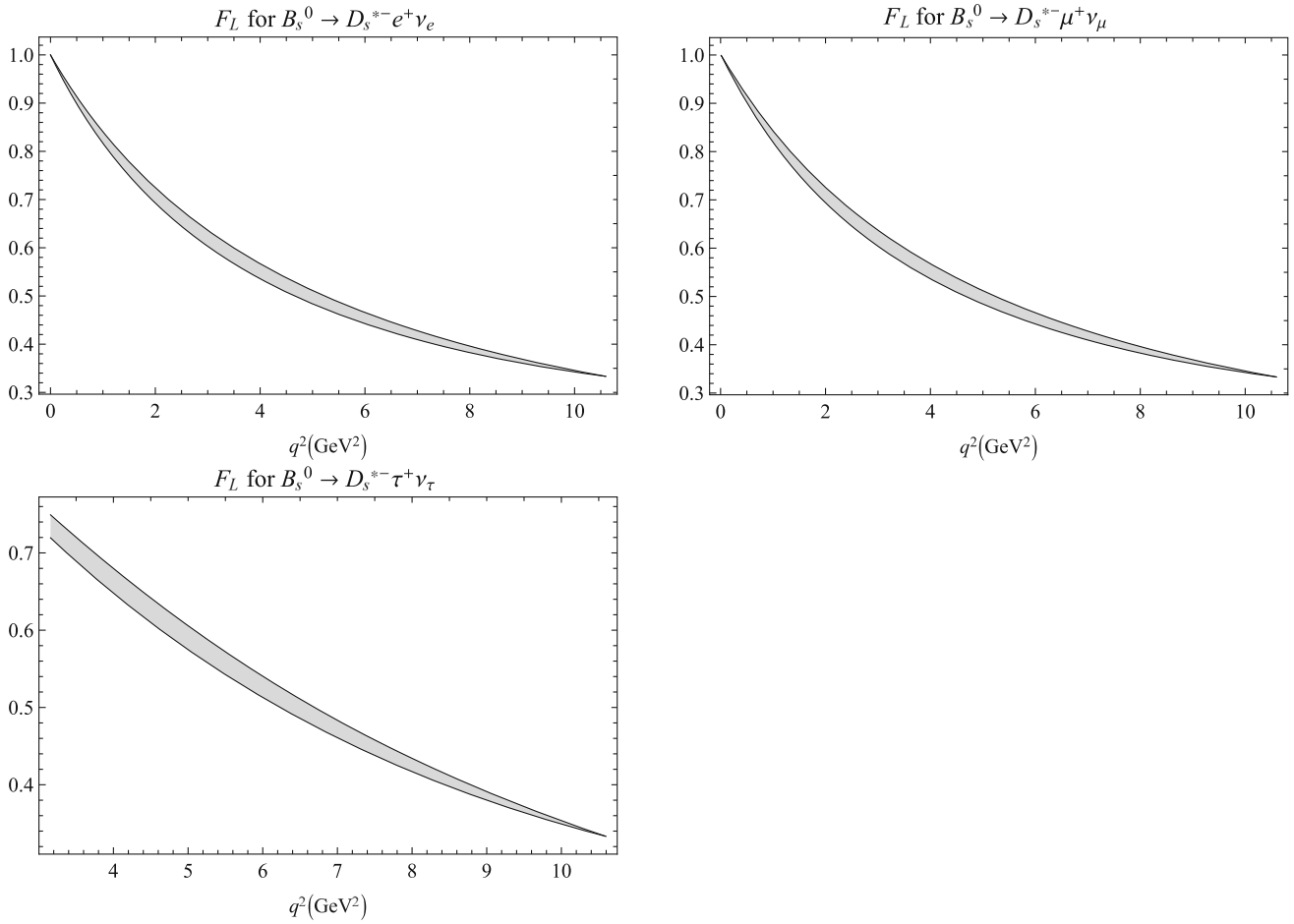

Fig. 6 Longitudinal polarization fraction for final state D_s^{*-} meson

with the available experimental data and lattice simulations. The same was also observed for studying the semileptonic decays of D and D_s mesons [31, 36, 39, 40].

5 Conclusion

In this article, we have studied a very interesting channel corresponding to the quark level transition $b \to c\ell^+\nu_\ell$. $B \to D^{(*)}\ell\nu_\ell$ have gained lot of attention, as some of its results deviate from the standard model predictions. Another channel $B_s^0 \to D_s^{(*)}\ell^+\nu_\ell$ has started getting attention after the first observation from the LHCb collaboration. Here, we compute the transition form factors for the channels $B_s \to D_s^-$ and $B_s^0 \to D_s^{-*}$ using the covariant confined quark model. We also compare our form factors with different other theoretical predictions including lattice simulations. We further compute different physical observables such as forward–backward asymmetry, lepton-side convexity parameter, and longitudinal and transverse polarizations along with their expectation values. Since these observables are yet to be examined from the experimental side, we compare only with the available theoretical prediction relativistic quark model. In general, all our results are in very good agreement with the available theoretical studies and lattice predictions.

Acknowledgements We would like to thank Prof. Mikhail A. Ivanov for useful discussions on some aspects of this work.

Data Availibility Statement There are no data associated with the manuscript.

References

1. J.A. Bailey et al., Phys. Rev. D **92**(3), 034506 (2015). https://doi.org/10.1103/PhysRevD.92.034506
2. H. Na, C.M. Bouchard, G.P. Lepage, C. Monahan, J. Shigemitsu, Phys. Rev. D **92**(5), 054510 (2015). https://doi.org/10.1103/PhysRevD.93.119906. (**Erratum: Phys. Rev. D 93, 119906 (2016)**)
3. Y. Li, C.D. Lü, Sci. Bull. **63**, 267 (2018). https://doi.org/10.1016/j.scib.2018.02.003

4. J. Albrecht, D. van Dyk, C. Langenbruch, Prog. Part. Nucl. Phys. **120**, 103885 (2021). https://doi.org/10.1016/j.ppnp.2021.103885
5. D. London, J. Matias, Ann. Rev. Nucl. Part. Sci. **72**, 37 (2022). https://doi.org/10.1146/annurev-nucl-102020-090209
6. R. Aaij et al., Phys. Rev. D **101**(7), 072004 (2020). https://doi.org/10.1103/PhysRevD.101.072004
7. E. McLean, C.T.H. Davies, J. Koponen, A.T. Lytle, Phys. Rev. D **101**(7), 074513 (2020). https://doi.org/10.1103/PhysRevD.101.074513
8. J. Harrison, C.T.H. Davies, Phys. Rev. D **105**(9), 094506 (2022). https://doi.org/10.1103/PhysRevD.105.094506
9. N. Penalva, J.M. Flynn, E. Hernández, J. Nieves, (2023)
10. G. Martinelli, M. Naviglio, S. Simula, L. Vittorio, Phys. Rev. D **106**(9), 093002 (2022). https://doi.org/10.1103/PhysRevD.106.093002
11. K. Azizi, Nucl. Phys. B **801**, 70 (2008). https://doi.org/10.1016/j.nuclphysb.2008.04.011
12. K. Azizi, M. Bayar, Phys. Rev. D **78**, 054011 (2008). https://doi.org/10.1103/PhysRevD.78.054011
13. M. Bordone, N. Gubernari, D. van Dyk, M. Jung, Eur. Phys. J. C **80**(4), 347 (2020). https://doi.org/10.1140/epjc/s10052-020-7850-9
14. Y. Zhang, T. Zhong, H.B. Fu, W. Cheng, L. Zeng, X.G. Wu, Phys. Rev. D **105**(9), 096013 (2022). https://doi.org/10.1103/PhysRevD.105.096013
15. R.N. Faustov, V.O. Galkin, Phys. Rev. D **87**(3), 034033 (2013). https://doi.org/10.1103/PhysRevD.87.034033
16. R.N. Faustov, V.O. Galkin, X.W. Kang, Phys. Rev. D **106**(1), 013004 (2022). https://doi.org/10.1103/PhysRevD.106.013004
17. O. Heger, M. Gómez-Rocha, W. Schweiger, Phys. Rev. D **104**(11), 116005 (2021). https://doi.org/10.1103/PhysRevD.104.116005
18. B.Y. Cui, Y.K. Huang, Y.M. Wang, X.C. Zhao, (2023)
19. R. Verma, J. Phys. G **39**, 025005 (2012). https://doi.org/10.1088/0954-3899/39/2/025005
20. H.Y. Xing, Z.N. Xu, Z.F. Cui, C.D. Roberts, C. Xu, Eur. Phys. J. C **82**(10), 889 (2022). https://doi.org/10.1140/epjc/s10052-022-10844-6
21. R. Dutta, N. Rajeev, Phys. Rev. D **97**(9), 095045 (2018). https://doi.org/10.1103/PhysRevD.97.095045
22. N. Das, R. Dutta, J. Phys. G **47**(11), 115001 (2020). https://doi.org/10.1088/1361-6471/aba422
23. N. Das, R. Dutta, Phys. Rev. D **105**(5), 055027 (2022). https://doi.org/10.1103/PhysRevD.105.055027
24. N.R. Soni, A. Issadykov, A.N. Gadaria, Z. Tyulemissov, J.J. Patel, J.N. Pandya, Eur. Phys. J. Plus **138**(2), 163 (2023). https://doi.org/10.1140/epjp/s13360-023-03779-8
25. G.V. Efimov, M.A. Ivanov, Int. J. Mod. Phys. A **4**(8), 2031 (1989). https://doi.org/10.1142/S0217751X89000832
26. G.V. Efimov, M.A. Ivanov, *The Quark Confinement Model of Hadrons* (IOP, Bristol, 1993)
27. M.A. Ivanov, P. Santorelli, Phys. Lett. B **456**, 248 (1999). https://doi.org/10.1016/S0370-2693(99)00474-8
28. T. Branz, A. Faessler, T. Gutsche, M.A. Ivanov, J.G. Korner, V.E. Lyubovitskij, Phys. Rev. D **81**, 034010 (2010). https://doi.org/10.1103/PhysRevD.81.034010
29. M.A. Ivanov, J.G. Korner, S.G. Kovalenko, P. Santorelli, G.G. Saidullaeva, Phys. Rev. D **85**, 034004 (2012). https://doi.org/10.1103/PhysRevD.85.034004
30. T. Gutsche, M.A. Ivanov, J.G. Korner, V.E. Lyubovitskij, P. Santorelli, Phys. Rev. D **86**, 074013 (2012). https://doi.org/10.1103/PhysRevD.86.074013
31. M.A. Ivanov, J.G. Körner, J.N. Pandya, P. Santorelli, N.R. Soni, C.T. Tran, Front. Phys. (Beijing) **14**(6), 64401 (2019). https://doi.org/10.1007/s11467-019-0908-1
32. A. Faessler, T. Gutsche, M.A. Ivanov, V.E. Lyubovitskij, P. Wang, Phys. Rev. D **68**, 014011 (2003). https://doi.org/10.1103/PhysRevD.68.014011
33. M.A. Ivanov, V.E. Lyubovitskij, Phys. Lett. B **408**, 435 (1997). https://doi.org/10.1016/S0370-2693(97)00776-4
34. A. Salam, Nuovo Cim. **25**, 224 (1962). https://doi.org/10.1007/BF02733330
35. S. Weinberg, Phys. Rev. **130**, 776 (1963). https://doi.org/10.1103/PhysRev.130.776
36. N.R. Soni, A.N. Gadaria, J.J. Patel, J.N. Pandya, Phys. Rev. D **102**, 016013 (2020). https://doi.org/10.1103/PhysRevD.102.016013
37. V.E. Lyubovitskij, A. Faessler, T. Gutsche, M.A. Ivanov, J.G. Korner, Prog. Part. Nucl. Phys. **50**, 329 (2003). https://doi.org/10.1016/S0146-6410(03)00026-7
38. M. Wirbel, B. Stech, M. Bauer, Z. Phys. C **29**, 637 (1985). https://doi.org/10.1007/BF01560299
39. N.R. Soni, J.N. Pandya, Phys. Rev. D **96**(1), 016017 (2017). https://doi.org/10.1103/PhysRevD.96.016017. (**Erratum: Phys. Rev. D 99, 059901 (2019)**)
40. N.R. Soni, M.A. Ivanov, J.G. Körner, J.N. Pandya, P. Santorelli, C.T. Tran, Phys. Rev. D **98**(11), 114031 (2018). https://doi.org/10.1103/PhysRevD.98.114031
41. N.R. Soni, J.N. Pandya, Springer Proc. Phys. **234**, 115 (2019). https://doi.org/10.1007/978-3-030-29622-3_16
42. N.R. Soni, J.N. Pandya, EPJ Web Conf. **202**, 06010 (2019). https://doi.org/10.1051/epjconf/201920206010
43. N.R. Soni, J.N. Pandya, Springer Proc. Phys. **261**, 85 (2021). https://doi.org/10.1007/978-981-33-4408-2_13
44. N.R. Soni, A. Issadykov, A.N. Gadaria, J.J. Patel, J.N. Pandya, Eur. Phys. J. A **58**(3), 39 (2022). https://doi.org/10.1140/epja/s10050-022-00685-y
45. N.R. Soni, A. Issadykov, A.N. Gadaria, J.J. Patel, J.N. Pandya, AIP Conf. Proc. **2377**(1), 090006 (2021). https://doi.org/10.1063/5.0063329
46. A. Issadykov, N. Soni, A. Gadaria, J. Patel, J.N. Pandya, PoS **PANIC2021**, 171 (2022). https://doi.org/10.22323/1.380.0171
47. M.A. Ivanov, J.G. Korner, P. Santorelli, Phys. Rev. D **63**, 074010 (2001). https://doi.org/10.1103/PhysRevD.63.074010
48. A. Faessler, T. Gutsche, M.A. Ivanov, J.G. Korner, V.E. Lyubovitskij, Eur. Phys. J. Direct **4**(1), 18 (2002). https://doi.org/10.1007/s1010502c0018
49. M.A. Ivanov, J.G. Korner, P. Santorelli, Phys. Rev. D **71**, 094006 (2005). https://doi.org/10.1103/PhysRevD.75.019901. (**Erratum: Phys. Rev. D 75, 019901 (2007)**)
50. M.A. Ivanov, J.G. Korner, P. Santorelli, Phys. Rev. D **73**, 054024 (2006). https://doi.org/10.1103/PhysRevD.73.054024

51. S. Dubnicka, A.Z. Dubnickova, A. Issadykov, M.A. Ivanov, A. Liptaj, Phys. Rev. D **96**(7), 076017 (2017). https://doi.org/10.1103/PhysRevD.96.076017
52. A. Issadykov, M.A. Ivanov, Phys. Lett. B **783**, 178 (2018). https://doi.org/10.1016/j.physletb.2018.06.056
53. S. Dubnička, A.Z. Dubničková, M.A. Ivanov, A. Liptaj, P. Santorelli, C.T. Tran, Phys. Rev. D **99**(1), 014042 (2019). https://doi.org/10.1103/PhysRevD.99.014042
54. S. Dubnička, A.Z. Dubničková, M.A. Ivanov, A. Liptaj, Phys. Rev. D **106**(3), 033006 (2022). https://doi.org/10.1103/PhysRevD.106.033006
55. M.A. Ivanov, Z. Tyulemissov, A. Tyulemissova, Phys. Rev. D **107**(1), 013009 (2023). https://doi.org/10.1103/PhysRevD.107.013009
56. G. Ganbold, T. Gutsche, M.A. Ivanov, V.E. Lyubovitskij, J. Phys. G **42**(7), 075002 (2015). https://doi.org/10.1088/0954-3899/42/7/075002
57. T. Gutsche, M.A. Ivanov, J.G. Körner, V.E. Lyubovitskij, P. Santorelli, N. Habyl, Phys. Rev. D **91**(7), 074001 (2015). https://doi.org/10.1103/PhysRevD.91.074001. (**Erratum: Phys. Rev. D 91, 119907 (2015)**)
58. L. Zhang, X.W. Kang, X.H. Guo, L.Y. Dai, T. Luo, C. Wang, JHEP **02**, 179 (2021). https://doi.org/10.1007/JHEP02(2021)179
59. M.A. Ivanov, J.G. Körner, C.T. Tran, Phys. Rev. D **92**(11), 114022 (2015). https://doi.org/10.1103/PhysRevD.92.114022
60. A. Issadykov, M.A. Ivanov, G. Nurbakova, EPJ Web Conf. **158**, 03002 (2017). https://doi.org/10.1051/epjconf/201715803002